RSC Advances

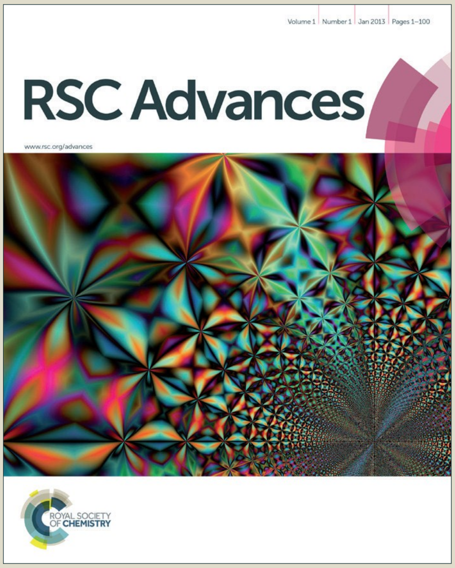

ROYAL SOCIETY
OF CHEMISTRY

www.rsc.org/advances

Conversion of Canola Oil and Canola Oil Methyl Ester (CME) to Green Aromatics over HZSM-5 Catalyst: A Comparative Study

A.Bayat, S.M. Sadrameli*

Chemical Engineering Department, Tarbiat Modares University

P.O. Box: 14115-143, Tehran, Iran

*Corresponding Author: Tel/Fax: +98 21 82884902

Email: sadramel@modares.ac.ir

Abstract

Catalytic conversion of canola oil and canola oil methyl ester (CME) for the production of green aromatics over HZSM-5 catalyst was investigated. General Factorial Design (GFD) of experiments was applied in order to evaluate the aromatics production statistically. The influence of reaction conditions such as reaction temperature and Weight Hourly Space Velocity (WHSV) on the yields of the aromatic products was studied in the experiments. The reaction temperatures were set at 375, 400, 450 and 500 °C whereas the space velocity was selected to be either 2 or 4 hr^{-1}. The products comprised of liquid hydrocarbon product (LHP), exhaust gases and water for both canola oil and CME. Moreover, thermal cracking of CME for the production of aromatics were conducted at temperatures of 450 and 500°C to compare the results with the corresponding catalytic route. The LHP was analyzed using Gas Chromatography (GC) to determine the BTX. Temperature, space velocity and feed type were found to be significant parameters for the production of aromatics. Comparison of CME and canola oil identified that catalytic cracking of CME leads to more aromatic production. Catalytic conversion of CME as well as canola oil yielded toluene as a major aromatic compound followed by para-meta xylenes and benzene. Thermal cracking of CME did not yield any aromatic products compared to the catalytic process.

Keywords: Catalytic conversion, Canola oil methyl ester, Green aromatics, HZSM-5, General Factorial Design

1. Introduction

Benzene, toluene, and xylenes (BTX) are among the very important aromatic products of chemical and petrochemical industry. These aromatics are produced during different processes. However, the most BTX production is achieved via catalytic reforming of naphtha which is a petroleum derivative.[1] Due to the depletion of conventional fossil energy resources such as petroleum, considerable attention has been devoted to the alternative renewable fuels that are environmentally friendly.[2-4] In this respect, vegetable oils have attracted much attention. Among the various methods for the conversion of vegetable oils to biofuels, catalytic cracking have been investigated by many researchers.[5-8] Canola oil as one of the vegetable oils has been converted to various hydrocarbons including aromatics, over different catalysts.[9-10]

On the other hand, Fatty Acid Methyl Esters (FAMEs) obtained via transesterification reaction of vegetable oil (triacylglycerol) with methanol have attracted remarkable attention due to different advantages they possess. The major benefits of FAMEs are renewability, environmentally benign nature, lubricity function, high cetane number, high flash point and biodegradability.[11] One of the major disadvantages of FAMEs that makes them thermally and chemically instable is the existence of oxygen in their molecular structure.[12] In order to overcome this drawback, deoxygenation of oxygen-containing molecules has been examined using zeolite catalysts at mild operating pressures.[12-14]

HZSM-5 catalyst has been applied for conversion of alcohols to hydrocarbons with high amount of aromatics.[15-16] Also, some research works have been allocated to conversion of oxygenate compounds like aldehydes, ketones and acids to hydrocarbons comprising of olefins and aromatics over HZSM-5.[17]

Conversion of methyl octanoate as a short chain methyl ester to hydrocarbons has been studied in the presence of HZSM-5.[18] The reaction of the methyl octanoate over HZSM-5 catalysts led to the production of various hydrocarbons consisting high amounts of aromatics.

In summary, although catalytic conversion of other types of oxygenates in the presence of HZSM-5 is extensively reported in the literature, it has been a few studies with conversion of fatty acid methyl esters (FAMEs). Hence, in this research work, conversion of canola oil and Canola Methyl Esters (CMEs) for the production of aromatics was studied and the results were discussed. Due to the previous reported studies in the literature regarding the possibility of aromatics production from thermal cracking of canola oil[19], thermal cracking of CME for aromatic production was conducted at two temperatures and the results were compared to the catalytic route.

2. Experimental

2.1. Materials

The ZSM-5 catalyst (CBV-5524G, SiO_2/Al_2O_3=50, NH_4 form) was supplied by Zeolyst Company. Prior to use, the as-received zeolite was calcined in air at 550 °C for 5 hours for converting to its hydrogen form. Methanol (99.8% purity) and potassium hydroxide (84% purity) were both obtained from Merck Company, Germany. Canola oil was provided from local market and utilized in the experiments without any purification. Fatty acids composition of the canola oil as determined by gas chromatography technique is presented in Table 1. CME was produced by conducting transesterification reaction between canola oil and methanol in the presence of potassium hydroxide catalyst. The temperature of the reaction, molar ratio of methanol to CME and catalyst content were found by preliminary experiments to be 60 °C, 6 and 0.6 weight percent of oil, respectively.

TABLE 1. CANOLA OIL FATTY ACIDS COMPOSITIONS

Fatty Acid	Structure	Content (wt. %)
Palmitic	**16:0**	**4**
Stearic	**18:0**	**4**
Oleic	**18:1**	**62**
Linoleic	**18:2**	**20**
Linolenic	**18:3**	**10**

2.2. *Catalyst Characterization*

The surface morphology of HZSM-5 catalyst depicting the size of crystals was characterized by Scanning Electron Microscopy (SEM) (KYKY-EM3200). The particle size distribution of the catalyst was measured using a Laser Fritsch Particle Sizer Analysette 22. Powder XRD (X-ray diffraction) pattern of the catalyst was recorded on a STOE Stadi MP diffractometer using Cu as an anode material at 40 kV and 30 mA (λ=1.54°A, scanning rate of 0.015 °/min in the 2θ range of 5-50). The acidity of the catalyst was measured by the method of NH3-TPD (Temperature-Programmed Desorption of Ammonia).

2.3. *Catalyst Activity*

The catalytic conversion of Canola Oil or CME to hydrocarbons was conducted in a continuous flow fixed-bed tubular reactor made of quartz with the inside diameter of 2 cm. The catalyst was placed over the thin layer of glass wool supported in a stainless steel grid centrally positioned within the reactor. The Process Flow Diagram of the experimental setup is illustrated in Figure 1. In order to study the influence of temperature and WHSV on aromatic content of liquid hydrocarbon product (LHP) and also aromatics yield, the reactor was operated at a temperature range of 375-500 °C and WHSV of 2 or 4. All experiments were performed under atmospheric pressure. Before initiation of the reaction, the temperature of the reactor was raised to 375, 400, 450 or 500 °C. Then the reactor was purged using nitrogen gas to remove the trapped oxygen inside the reactor. Thereafter, the canola oil or CME was introduced to the reactor at a predetermined space velocity and after vaporization in the primary section of the reactor, reacted over the catalyst bed. The outlet product vapor passed through water-cooled and ice-cooled condensers consecutively to condense the vapors as far as possible. The products mainly comprised of water, liquid hydrocarbon product (LHP) and exhaust gases. The LHP obtained by catalytic cracking of canola oil and CME, were called LHPO and LHPM, respectively. Thermal cracking of CME was also done in the aforementioned experimental setup. The thermal cracking experiments were conducted at 450 and 500 °C and 2 hr^{-1} WHSV. Although instead of catalyst particles, the center of the tubular reactor was filled with inert pellets to increase the surface area for thermal cracking reactions.

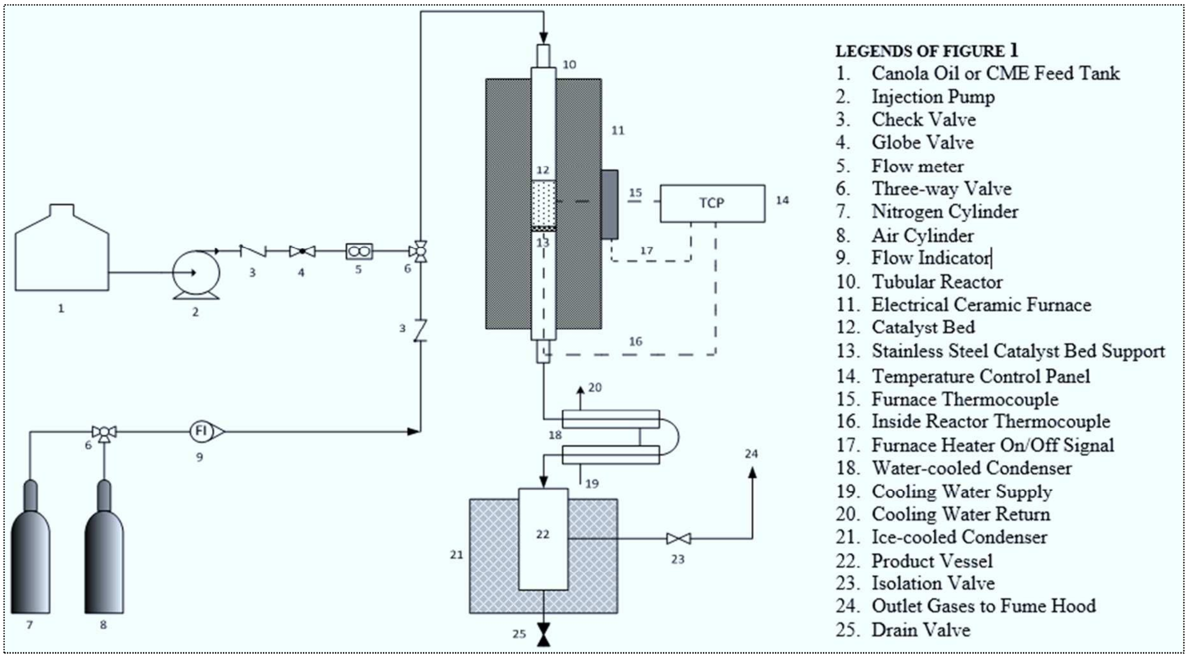

FIGURE 1. PROCESS FLOW DIAGRAM OF GREEN AROMATICS PRODUCTION

2.4. Design of Experiments

General Factorial Design (GFD) was applied to study the influence of temperature and space velocity on the aromatic yield. When using GFD, It's possible to have parameters with different number of levels. The GFD includes all possible combinations of the factor levels. Additionally, one of the major applications of GFD is the possibility of analyzing mixtures of categorical and numeric factors simultaneously. In this research, Design Expert software (version 7.1.3) was employed to design the experiments and analyze the results statistically. Temperature and WHSV was selected as independent numeric parameters. The reactant type, namely CME or canola oil was chosen as categorical factor. The total aromatic content measured from LHP analysis was the response factor. Table 2 shows the levels of the variables investigated in this study.

TABLE 2. LEVELS OF THE SELECTED VARIABLES

Factor	Unit	Low Level	Intermediate Levels		High Level
Reaction Temperature	°C	375	400	450	500
WHSV	hr^{-1}	2		4	
Feed Type	Categorical Factor	Canola Oil and CME			

2.5. Analysis of Product

In order to identify the amounts of aromatic hydrocarbons in the LHP, a Varian CP-3800 gas chromatograph equipped with a Flame Ionization Detector (FID) was used. The GC column was CP-Sil 13 CB with 25 m length, 0.53 mm I.D. and 0.2 µm film thickness. The temperature of the column oven was programmed to maintain at 80 °C for 12 min, then increased to 250 °C with the rate of 30 °C/min and hold at 250 °C for 13 minutes. Equations 1 and 2 describe the LHP yield and aromatic yield consecutively:

$$\text{LHP Yield (\%)} = 100 \times (\text{Mass of LHP (g)}) / (\text{Mass of the Canola Oil or CME Feed (g)}) \quad (1)$$

$$\text{Aromatic Yield (wt. \%)} = (\text{Aromatic Content (wt. \%)}) \times (\text{LHP Yield (wt. \%)}) \quad (2)$$

Moreover, as the BTX boiling points are in the range of 70-160, the LHP was distilled into three boiling ranges of less than 70, 70-160 and 160+ °C to roughly estimate the cut of the product which comprised of BTX.[20]

3. Results and Discussion

3.1. Catalyst Characterization

SEM image of ZSM-5 catalyst is depicted in Figure 2. The electron micrographs exhibited that the catalyst particles were in the micrometer scale.

Particle size distribution of the catalyst is shown in Figure 3. Q3(x) is the percentage of the complete sample volume filled with particles smaller than x µm while dQ3(x) corresponds to the volume percentage of the sample particles with diameters between x and y µm. As displayed, almost 80% of the particle sizes are in the range of 0.1-0.5 µm. The arithmetic mean diameter of particles as measured by the particle size analysis method, is 1.17 µm.

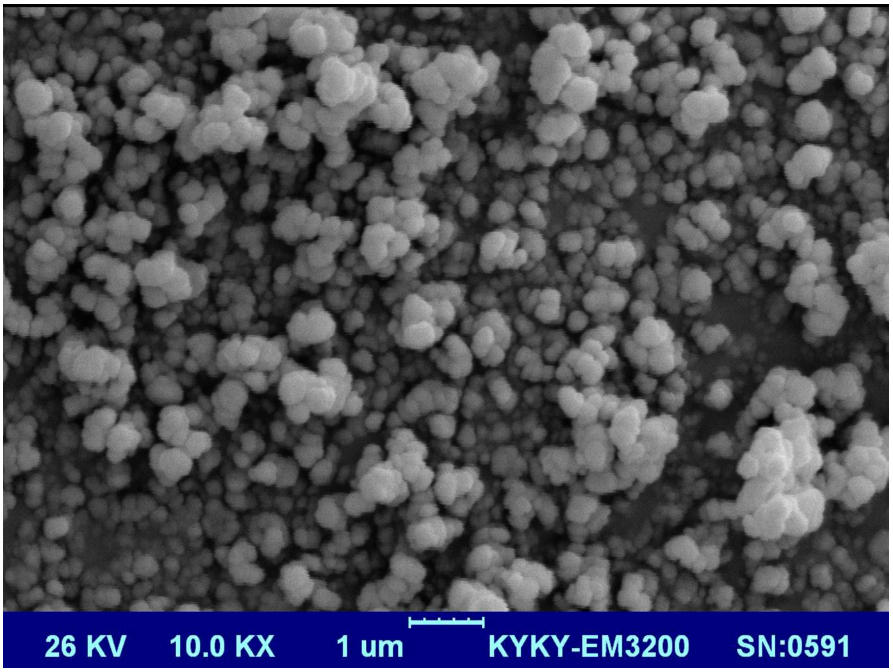

FIGURE 2.SEM IMAGE OF THE HZSM-5 CATALYST APPLIED IN THE EXPERIMENTS

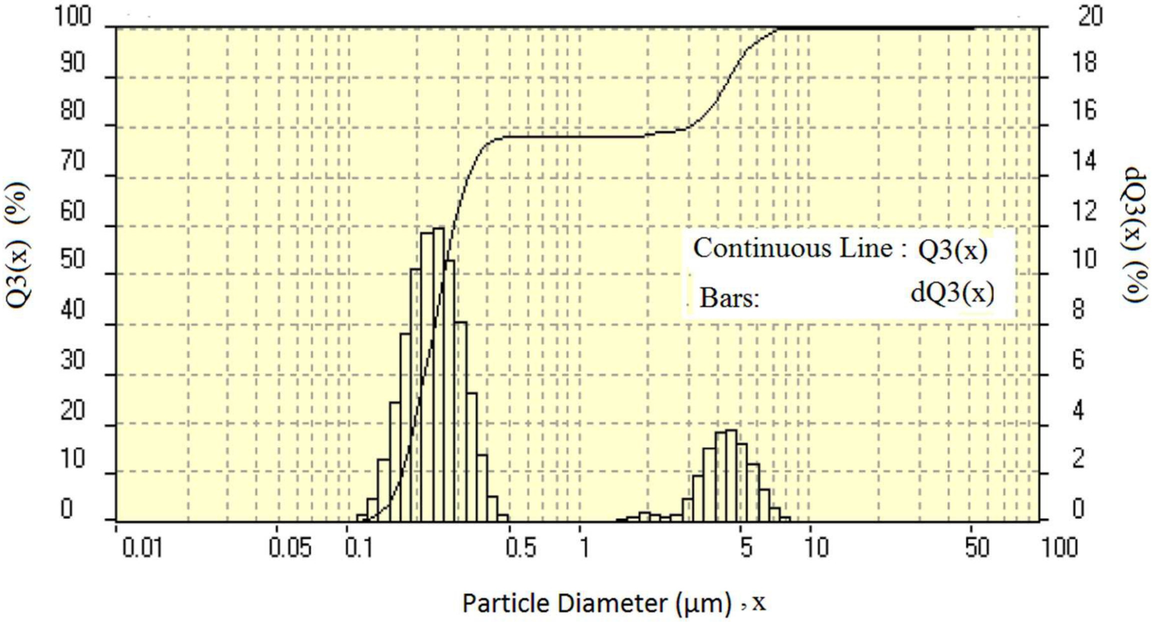

FIGURE 3. PARTICLE SIZE DISTRIBUTION OF HZSM-5 CATALYST

The XRD pattern of the catalyst as shown in Figure 4 comprises of peaks in the 2θ ranges of 7-10 and 20-25 nm in agreement with the previous studies in the literature.[21-22]

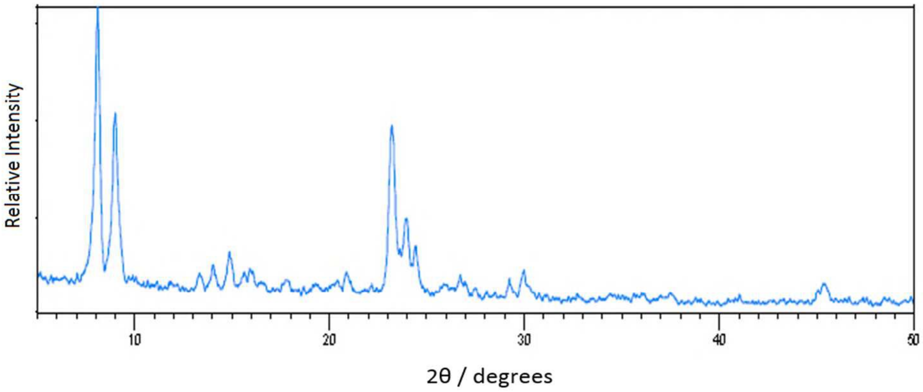

FIGURE 4. XRD PATTERN OF THE ZSM-5

Figure 5 shows acid site distribution of ZSM-5 catalyst as determined by TPD of ammonia. The catalyst indicates three desorption peaks at 230, 428 and 659 °C which can be attributed to the NH_3 desorbed from the low, medium and high strengths acid sites, respectively. The total acid sites of ZSM-5 as measured by TPD was 1.14 mmol NH_3/g.

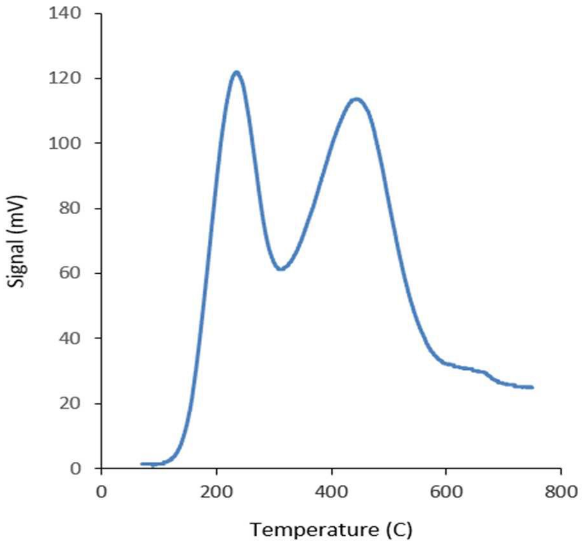

FIGURE 5. NH3-TPD PROFILE OF THE ZSM-5 CATALYST

3.2.Design of Experiments (DOE) and Analysis of Variance (ANOVA)

The experimental design layout as well as responses is presented in Table 3. In order to fit the experimental points, a modified quadratic model was suggested. Estimation models of aromatic yields for canola oil and CME in terms of actual factors are indicated respectively by Equations 3 and 4.

$$\text{Aromatic Yield} = -185.90594+1.16001 * \text{Temperature}-31.24879 * \text{WHSV}+0.057041 * \text{Temperature} * \text{WHSV}-1.44554\text{E-}003 * \text{Temperature}^2 \quad (3)$$

$$\text{Aromatic Yield} =-190.25344+1.16001 * \text{Temperature}-27.35129 * \text{WHSV}+0.057041 * \text{Temperature} * \text{WHSV} -1.44554\text{E-}003 * \text{Temperature}^2 \quad (4)$$

TABLE 3. EXPERIMENTAL DESIGN STRUCTURE AND THE RELATED RESPONSES

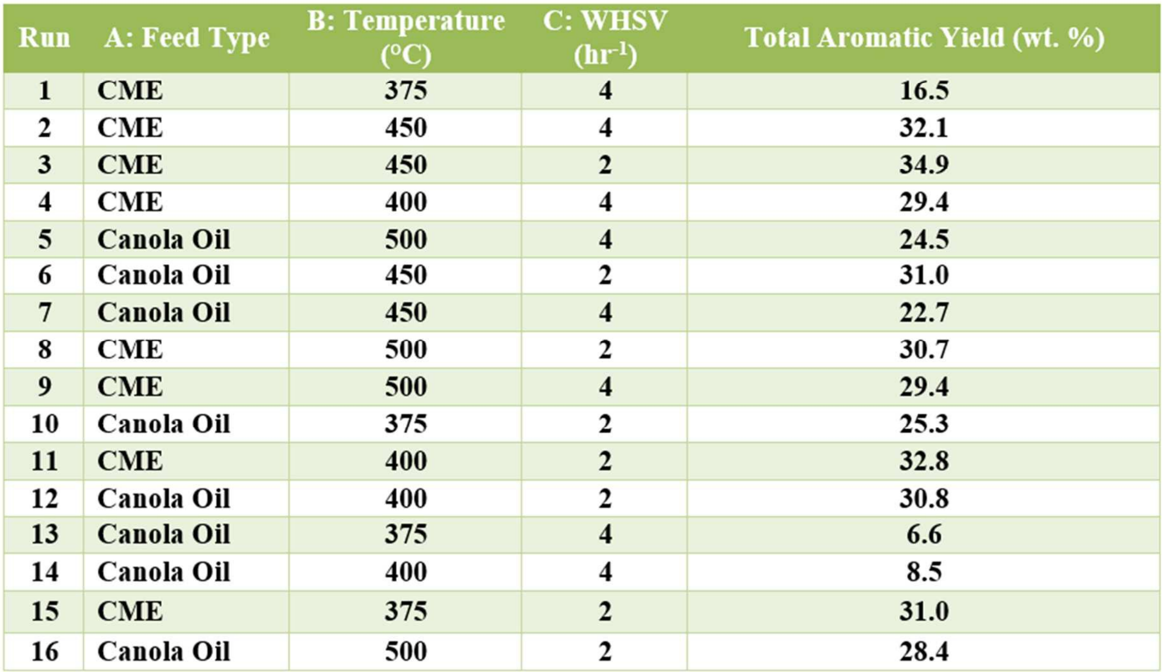

Run	A: Feed Type	B: Temperature (°C)	C: WHSV (hr^{-1})	Total Aromatic Yield (wt. %)
1	CME	375	4	16.5
2	CME	450	4	32.1
3	CME	450	2	34.9
4	CME	400	4	29.4
5	Canola Oil	500	4	24.5
6	Canola Oil	450	2	31.0
7	Canola Oil	450	4	22.7
8	CME	500	2	30.7
9	CME	500	4	29.4
10	Canola Oil	375	2	25.3
11	CME	400	2	32.8
12	Canola Oil	400	2	30.8
13	Canola Oil	375	4	6.6
14	Canola Oil	400	4	8.5
15	CME	375	2	31.0
16	Canola Oil	500	2	28.4

The Design Expert software was used to analyze the suggested model statistically, evaluate the ANOVA and check the suitability of the model as illustrated in Table 4.

TABLE 4. ANALYSIS OF VARIANCE FOR THE MODEL

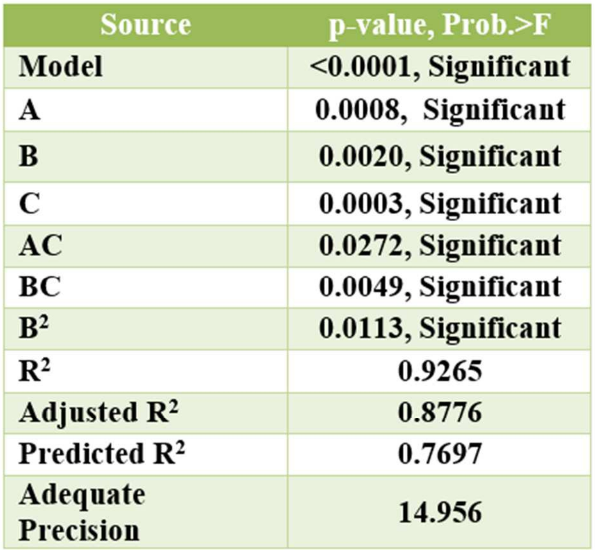

Source	p-value, Prob.>F
Model	<0.0001, Significant
A	0.0008, Significant
B	0.0020, Significant
C	0.0003, Significant
AC	0.0272, Significant
BC	0.0049, Significant
B^2	0.0113, Significant
R^2	0.9265
Adjusted R^2	0.8776
Predicted R^2	0.7697
Adequate Precision	14.956

According to Table 4, the model p-value was less than 0.0001, indicating high significance in predicting the values of response. The AB and C^2 were insignificant model terms that were removed from the model. The other model terms as shown in Table 4 are significant.

The R-Squared which is also known as the coefficient of determination, is the measure of how close the response values are to the fitted model equations. The R-Squared was calculated to be 0.9265 for the response. This value implies that 92.65% of the experimental data were consistent with the model predicted data.

The "Predicted R-Squared" of 0.7697 was close to the "Adjusted R-Squared" of 0.8776. The difference between these values should be lower than o.2 to conclude that there is no problem with the model or the data.

The "Adequate Precision" of more than 4 is acceptable. Therefore, the value of 14.956 shows an adequate signal.

Figure 6 shows the predicted values of total aromatic yields (by the model equations 3 and 4) versus actual experimental data. As illustrated, the predicted responses are in good agreement with the observed experimental values.

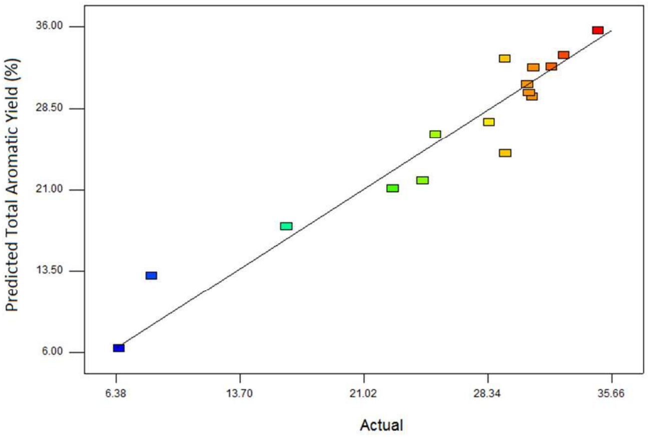

FIGURE 6.PREDICTED TOTAL AROMATICS YIELD VS. ACTUAL VALUES

3.3.Catalytic activity in aromatic hydrocarbons production

3.3.1. The effect of reaction conditions on LHP yield

Yields of LHPs (LHPO and LHPM) at different operating conditions are illustrated in Figure 7. Elevating in temperature, causes more cracking reactions, leading to production of more light gases. Hence as expected, with raising in temperature, both LHPO and LHPM yields decreased.

The higher the space velocity, the lower is the residence time of hydrocarbons in the reaction medium. So, due to less residence time, lower light gases formed and consequently, the yields reasonably increased.

In comparison with CME, because of the fact that canola oil (triacylglycerol molecules) has heavier molecules, it’s cracking needs for more severe operating conditions. Therefore, the yield of LHPO was higher than LHPM yield at the same temperatures and space velocities.

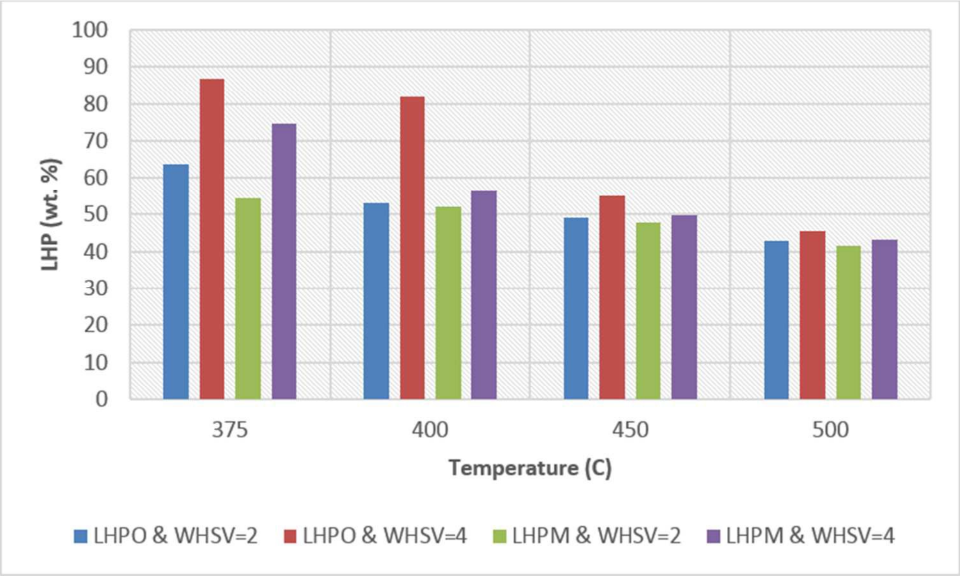

FIGURE 7.LHPO AND LHPM YIELDS AT DIFFERENT OPERATING CONDITIONS

3.3.2. The effect of reaction conditions on distillation cuts of LHP

Figure 8 depicts the comparison between the LHPO and LHPM distillation cuts at different operating conditions. As illustrated, the weight fraction of cut with boiling point range of 70-160 increased with raising in the temperature and/or reduction in the space velocity whereas the heavier “160+ cut” and “below 70 cut” weight fractions were decreased. This phenomenon was ascribed to more cracking reactions at higher temperatures and/or lower space velocities leading to lighter hydrocarbons with lower boiling point. In contrast with LHPO, the weight fraction of 70-160 boiling cut of LHPM was higher and portion of its heavier components (160+ boiling point cut) was lower. It can be explained such that the lighter the molecules of the inlet feed to the reactor, the higher was the light fraction of the LHP.

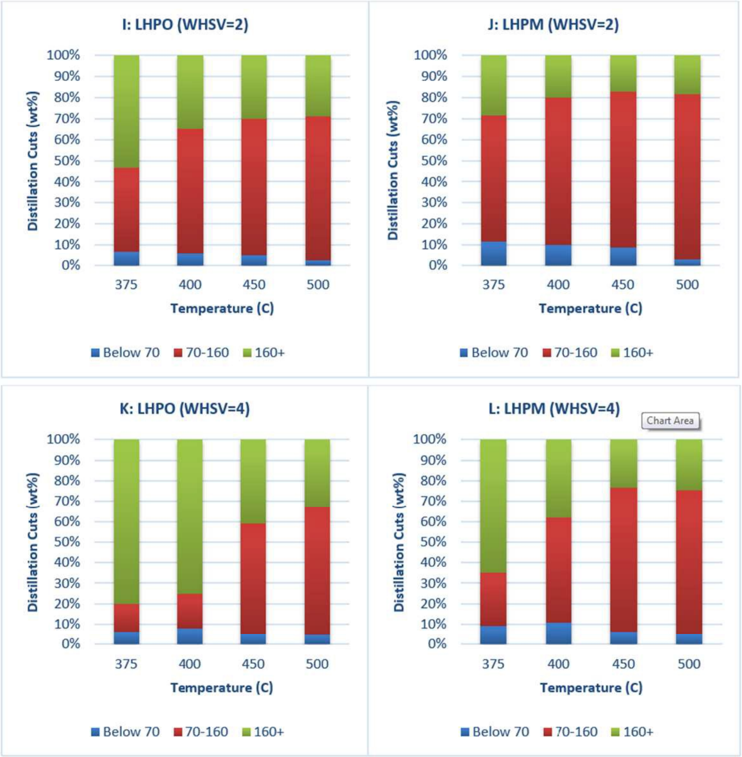

FIGURE 8: COMPARISON OF LHPO AND LHPM DISTILLATION CUTS (I-L)

3.3.3. The effects of reaction conditions on aromatics production

Figure 9 depicts the total aromatic contents of LHPO and LHPM at different reaction conditions as determined by GC analysis. According to the figure, the total aromatic content was increased with raising in the temperature and/or lowering the space velocity. As mentioned in the literature, [9] the required reactions for oxygenate (methyl ester or vegetable oil) conversion include thermal-catalytic cracking and deoxygenation. Complementary reactions that convert the produced hydrocarbons to aromatics comprise of oligomerization, acid catalyzed cyclization and H-transfer. Cracking and deoxygenation are occurred on Bronsted and Lewis acid sites. HZSM-5 includes acid sites to conduct the above reactions and also secondary cracking, olefin oligomerization, cyclization and H-transfer which are essential steps to produce aromatic hydrocarbons.[9, 23] A different path that have been presented for methyl ester aromatization, includes intermediate compounds produced during the conversion of oxygenate. These intermediates represent strong interaction with the catalysts.[18] The aforementioned intermediates, due to their low mobility, remain on the catalyst surface as long as to be converted to aromatics especially while the space velocity is 2 hr^{-1}. Additionally, the lower the space velocity, the higher is the space time for olefin oligomerization and cyclization reactions, leading to aromatic production. The total aromatic content of LHPM was higher than LHPO at the same operating conditions. Difference between aromatic content of LHPO and LHPM was more significant when the space velocity was 4 hr^{-1}. It can be explained that cracking is one of the major and primary steps for aromatization of oxygenates. The higher aromatic content of LHPM may be attributed to more cracking reactions of CME because it consists of lighter molecules. The total aromatic content increased with raising in the temperature and reached to its maximum at approximately 450 °C. This trend is true for all operating conditions except when the space velocity of canola oil is 4 hr^{-1}. In this case, the maximum total aromatic content of LHPO was obtained at 500 °C. This may be due to increasing the cracking reactions of higher molecular weight canola oil at elevated temperatures that enhanced aromatization of the oil.

Besides, total aromatic yields were calculated using Equation 2. Figure 10 demonstrates total aromatic yields at different operating conditions. According to this figure, the total aromatic yields were increased with raising in the temperature to its maximum value and then decreased. Further cracking of cracked methyl esters to light gases at higher temperatures may cause diminishing of total aromatic yield. The exception of this trend is the case of LHPO at 4 hr^{-1} space velocity. The reason of this phenomenon may be more cracking of the oil and enhancement of aromatization at elevated temperatures.

The effect of interaction between reaction temperature and space velocity for both canola oil and CME is depicted in 3D plots of Figure 11. As displayed, the total aromatic yield was increased with raising in the temperature and decreasing the space velocity. Increasing the temperature further than 450 °C caused the total aromatic yield to decrease. Therefore, operation at such high temperatures is not reasonable.

Yields of aromatic hydrocarbon products are provided in Table 5. BTX which are critical aromatics had relatively high yields as shown in the table. Also, both feeds had similar distribution of aromatic products. The affinity to the production of C7-C9 aromatics was related to shape selectivity of HZSM-5 catalyst.[23] Toluene was the main aromatic hydrocarbon produced followed by Para-meta xylenes, benzene and Ortho-xylene.

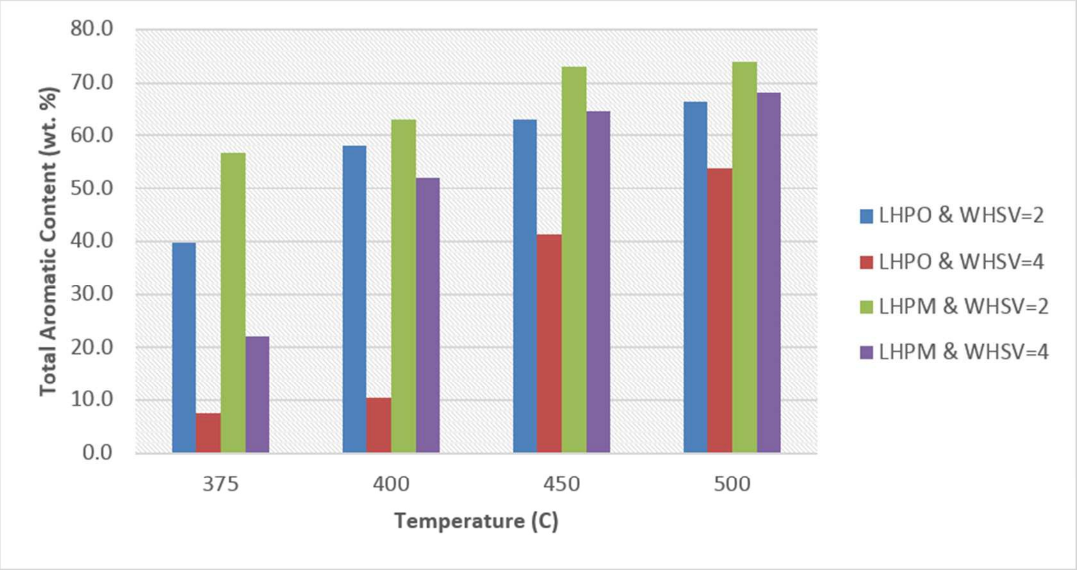

FIGURE 9. TOTAL AROMATIC CONTENT OF LHPO AND LHPM AT DIFFERENT REACTION CONDITIONS

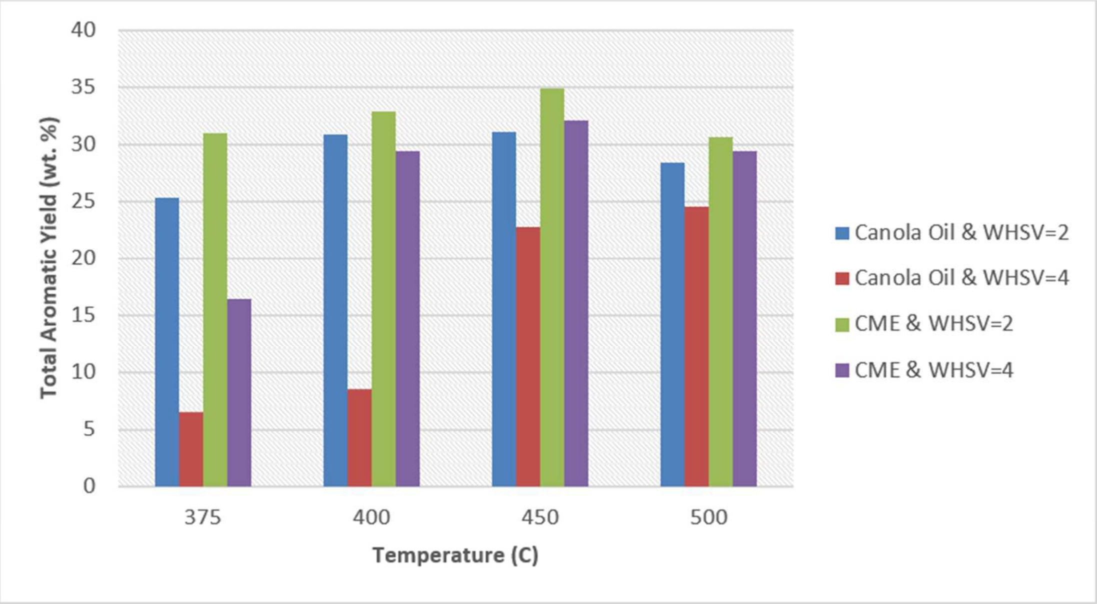

FIGURE 10.TOTAL AROMATIC YIELDS AT DIFFERENT REACTION CONDITIONS

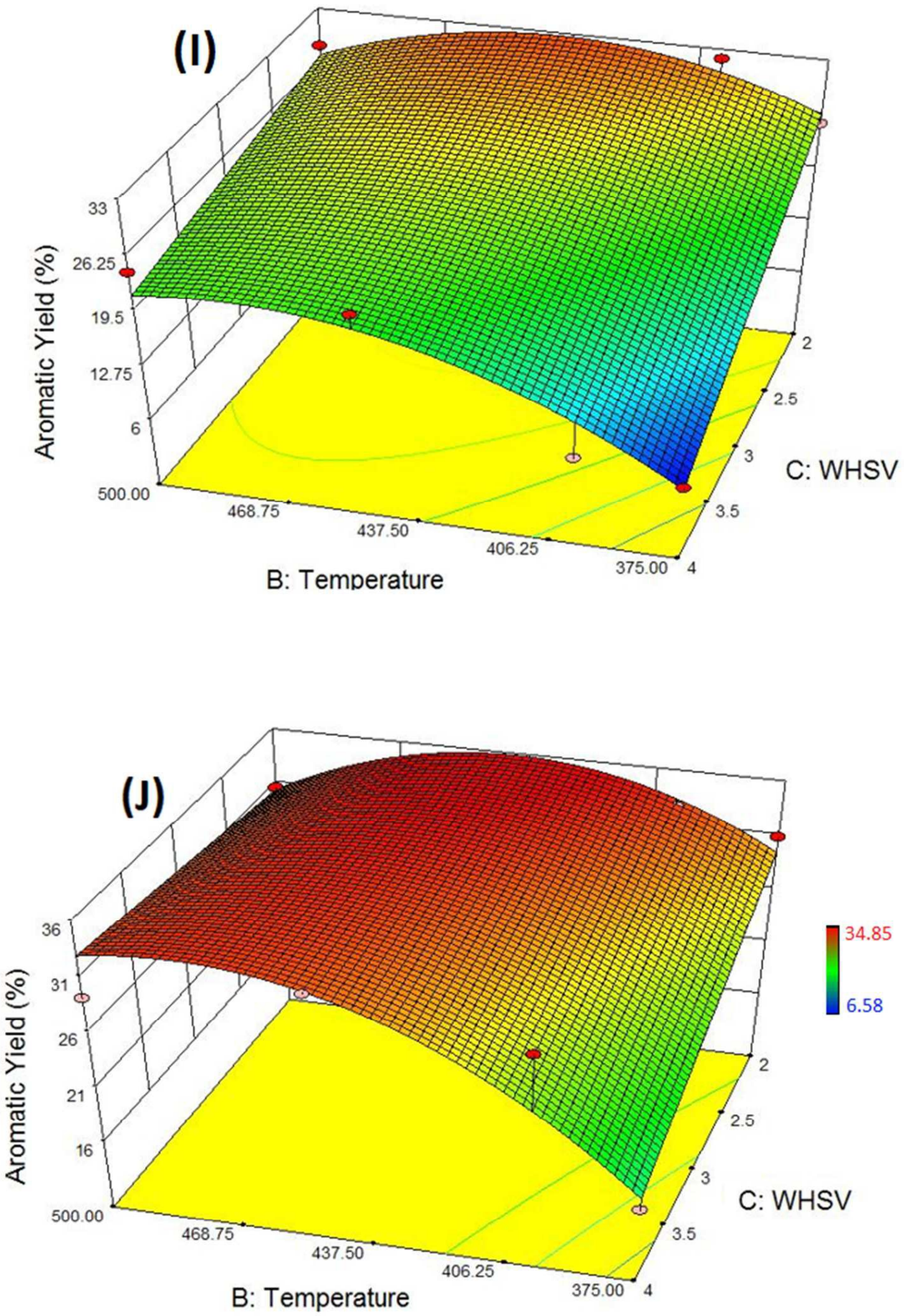

FIGURE 11. 3D PLOTS OF PREDICTED AROMATIC YIELD VERSUS TEMPERATURE AND WHSV FOR CANOLA OIL (I) AND CME (J)

TABLE 5. YIELDS OF AROMATIC HYDROCARBONS AT DIFFERENT OPERATING CONDITIONS

Feed	WHSV	Temperature	Benzene	Toluene	Para-Meta Xylene	Ortho Xylene	C9 Aromatics
Canola Oil	2	375	2.27	7.89	6.21	1.66	7.27
		400	3.26	10.95	7.75	2.23	7.71
		450	3.76	11.51	8.03	2.46	5.31
		500	4.33	11.93	6.98	2.23	2.99
	4	375	0.57	1.72	1.57	0.37	2.39
		400	0.67	2.19	2.04	0.49	3.14
		450	1.97	6.6	5.98	1.6	6.62
		500	2.65	8.67	6.84	2.06	4.31
CME	2	375	2.34	9.43	8.61	2.62	8.02
		400	2.97	10.26	8.39	3.02	8.18
		450	3.48	11.77	9.82	3.24	6.53
		500	4.31	12.56	7.92	2.57	3.31
	4	375	1.12	4.1	4.25	1.04	6.03
		400	3.72	10.54	7.27	1.92	5.86
		450	4.73	12.05	8.07	2.29	5.02
		500	4.35	11.64	7.54	2.41	3.36

3.3.4. Thermal cracking of CME for aromatic production

The CME thermal cracking results is represented in Table 6. As shown, increasing in the temperature caused more aromatic production. However, the aromatic yield through thermal cracking was very low in comparison with the catalytic cracking route. In conclusion, thermal cracking of CME is not adequate solitarily for aromatics production and presence of catalyst to enhance the yields is essential.

TABLE 6.TOTAL AROMATIC CONTENT AND YIELD OF CME THERMAL CRACKING

Temperature (°C)	LHP (wt. %)	Total Aromatic Content (wt. %)	Total Aromatic Yield (wt. %)
450	93.6	0.7	0.66
500	74.9	2.3	1.7

4. Conclusions

Conversion of canola oil and CME to aromatic rich hydrocarbons was conducted in the presence of HZSM-5 catalyst. Influences of reaction temperature and space velocity on the production of aromatics from canola oil and CME were investigated using General Factorial Design (GFD). Reaction temperature, space velocity and feed type were found as significant parameters in aromatic production. In comparison with canola oil, catalytic cracking of CME yielded more amounts of aromatics. The difference between aromatic yields of canola oil and CME was more pronounced at higher space velocities. The maximum amount of aromatic yield was obtained at temperature of 450 $^{\circ}$C and space velocity of 2 hr^{-1}. Further increasing the temperature led to loss of aromatic yield for both feeds. The distribution of aromatic products was similar for both canola oil and CME. The main aromatic product of the process was toluene followed by para-meta xylene and benzene. Thermal cracking of the CME yielded minor amounts of aromatics that could not compete to catalytic route for aromatic production.

Acknowledgment

This contribution was based on the research supported by grant from Tarbiat Modares University.

References

[1] M.R. Rahimpour, M. Jafari, D. Iranshahi, *Appl. Energy*, 2013, **109**, 79–93.

[2] P.S. Rezaei, H. Shafaghat, W.M.A.W. Daud, *App. Cat. A: Gen.*, 2014, **469**, 490-511.

[3] L. Wang, H. Lei, Q. Bu, S. Ren, Y. Wei, L. Zhu, X. Zhang, Y. Liu, G. Yadavalli, J. Lee, S. Chen, J. Tang, *Fuel*, 2014, **129**, 78-85.

[4] B. Zhang, Z. Zhong, K. Ding, Z. Song, *Fuel*, 2015, **139**, 622-628.

[5] P. Tamunaidu, S. Bhatia, *Bioresour. Technol.*, 2007, **98**, 3593–3601.

[6] C.M.R. Prado, F.N.R. Antoniosi, *J. Anal. Appl. Pyrolysis*, 2008, **86**, 338–347.

[7] H. Li, P. Yu, B. Shen, *Fuel Process. Technol.*, 2009, **90**, 1087–1092.

[8] H. Li, B. Shen, J.C. Kabalu, M. Nchare, *Renew. Energy*, 2009, **34**, 1033–1039.

[9] S.P.R. Katikaneni, J.D. Adjaye, N.N. Bakhshi, *The Can. J. of Chem. Eng.*, 1995, **73**, 484-497.

[10] S.M. Sadrameli, A.E.S. Green, W. Seames, *J. Anal. Appl. Pyrolysis*, 2009, **86**, 1-7.

[11] N. Pasupulety, K. Gunda, Y. Liu, G.L. Rempel, F.T.T. Ng, *Appl. Catal. A: Gen.*, 2013, **452**, 189-202.

[12] T. Sooknoi, T. Danuthai, L.L. Lobban, R.G. Mallinson, D.E. Resasco, *J. of Catal.*, 2008, **258**, 199-209.

[13] R. Cerny, M. Kubu, D. Kubicka, *Catal.Today*, 2013, **204**, 46-53.

[14] T. Danuthai, T. Sooknoi, S. Jongpatiwut, T. Rirksomboon, S. Osuwan, D.E. Resasco, *Appl. Catal. A: Gen.*, 2011, **409-410**, 74-81.

[15] J.D. Adjaye, N.N. Bakhshi, *Fuel Process. Technol.*, 1995, **45**, 161-183.

[16] A.A. Rownaghi, F. Rezaei, J. Hedlund, *Microporous and Mesoporous Mater.*, 2012, **151**, 26-33.

[17] A.G. Gayubo, A.T. Aguayo, A. Atutxa, R. Aguado, M. Olazar, J. Bilbao, *Ind. Eng. Chem. Res.*, 2004, **43**, 2619-2626.

[18] T. Danuthai, S. Jongpatiwut, T. Rirksomboon, S. Osuwan, D.E. Resasco, *Appl. Catal. A: Gen.*, 2009, **361**, 99-105.

[19] O.I. Raphael, S.P.R. Katikaneni, N.N. Bakhshi, *Energy & Fuels*, 1996, **10**, 1150-1162.

[20] R.C. Weast, M.J. Astle, W.H. Beyer, *CRC handbook of Chemistry and Physics*, 69th ed., CRC Press. Florida, USA, 1988-1989.

[21] Y. Cheng, L.J. Wang, J.S. Li, Y.C. Yang, X.Y. Sun, *Mater. Lett.*, 2005, **59**, 3427-3430.

[22] M. Khatamian, M. Irani, *J. of the Iran. Chem. Soc.*, 2009, **6**, 187-194.

[23] N.Y. Chen, W.E. Garwood, F.G. Dwyer, *Shape Selective Catalysis in Industrial Applications*. Marcel Dekker, New York, USA, 1989.